74275

DRAFT

Oriented high-Ti Basalt

1493 grams

Introduction

74275 is a fine-grained, high-Ti mare basalt with significant armalcolite content (Hodges and Kushiro 1974; Neal and Taylor 1993). It contains vesicles, vugs and unusual olivine megacrysts (Fo_{82}) (Meyer and Wilshire 1974).

74275 was collected from the rim of Shorty crater and was photographed both on the lunar surface and in the laboratory (with similar lighting) to document the exact lunar orientation. (Wolfe et al. 1981). This sample has proven useful to studies that require known lunar orientation with extended exposure history to the extra-lunar environment (micrometeorites, cosmic rays, solar irradiation). The sample is relatively flat 17 by 12 cm and 4 cm thick. The top (T_1) surface is somewhat rounded and has many micrometeorite pits (figure 2), while the bottom (B_1) surface is flat and angular and without any evidence of exposure to the micrometeorites (figure 3). Fink et al. (1998) have carefully considered the exact orientation (30 deg tilt), shielding (nearby boulder) and detailed exposure history (complex) of 74275.

This basalt has been determined to be very old (> 3.8 b.y.).

Petrography

Perhaps the best petrographic description of 74275 is given by Hodges and Kushiro (1974): *"Rock 74275 is a fine-grained ilmenite basalt with microphenocrysts of olivine (Fo_{80-71}), titanaugite (up to 6.8 wt. % TiO_2) and armalcolite rimmed with ilmenite set in a subvariolitic groundmass of clinopyroxene, plagioclase (An_{88-78}), ilmenite, tridymite, metallic iron (Ni<1 wt.%), troilite and glass. Spinel occurs only within olivine grains."*

Neal and Taylor (1993) and Brown et al. (1975) compare 74275 with a suite of high-Ti basalts from Apollo 17. 74275 contains groundmass plagioclase, pyroxene and ilmenite with larger crystals of pink pyroxene (up to 0.5 mm) and olivine (up to 0.7 mm) and ilmenite/armalcolite laths (up to 0.7 mm in length) (figure 5). Pyroxene rims are present on some olivine phenocrysts. Minor blebs of iron metal and troilite are found in the mesostasis. Olivine megacrysts (figure 6), some termed "dunite inclusions", are common in 74275 (Meyer and Wilshire 1974). These can be seen as green inclusions in the photo of the bottom surface (figure 3).

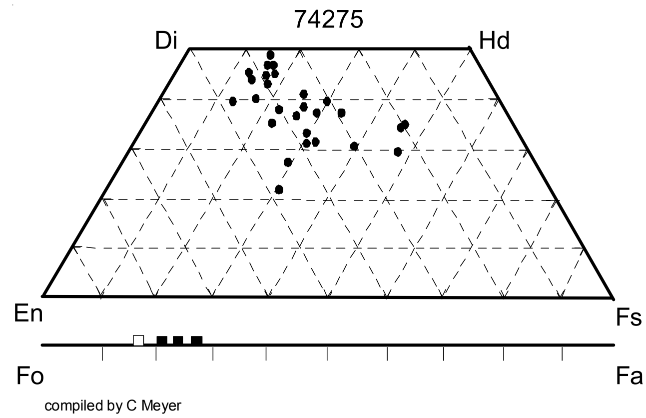

Figure 1: Composition of pyroxene and olivine in 74275 (replotted from Hodges and Kushiro 1974, with apologies). The open symbol at Fo_{82-84} represents the composition of olivine xenocrysts (Delano and Lindsley 1982).

Mineralogy

Pyroxene: The pyroxenes in 74275 are high Ca pyroxene without the presence of low-Ca pyroxene (figure 1). Sung et al. (1974) have shown that the pyroxenes in 74275 contain high concentrations of Ti^{3+}.

Olivine: Delano and Lindsley (1982) have carefully considered the olivine in 74275 (figure 5). The olivine megacrysts in 74275 are too magnesium rich to have formed from the melt (Meyer and Wilshire 1974).

Mineralogical Mode

	Brown et al. 1975	**Meyer and Wilshire 1974**
Olivine	13 %	16.1
Pyroxene	36	34.9
Opaques	31	33.3
Plagioclase	19	15.6

Figure 2: Top surface of 74275 showing numerous micrometeorite "zap" pits. NASA# S73-16018. Cube is 1 cm.

Figure 3: Bottom surface of 74275 showing vesicles and vugs. NASA# S73-16019 (fadded). Cube is 1 cm.

Figure 4: Photomicrograph of thin section of 74275 (from Neal and Taylor 1993).

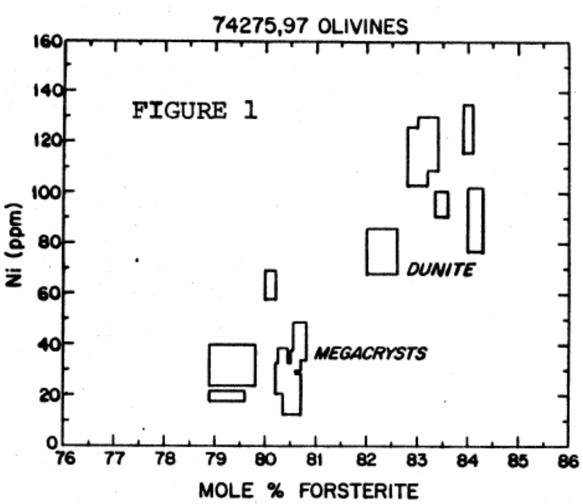

Figure 5: Ni and Mg in olivine in 74275 (from Delano and Lindsley 1982).

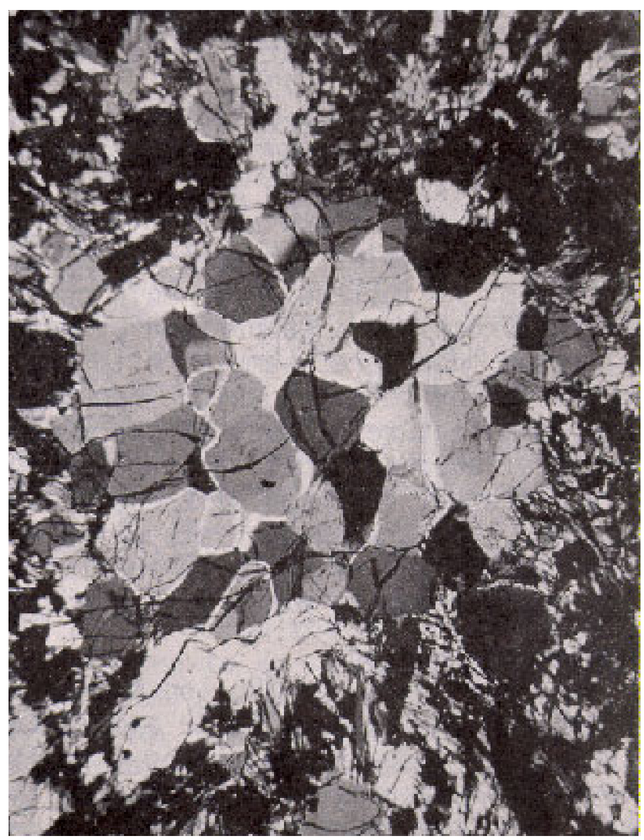

Figure 6: Photomicrograph of "dunite" inclusion in 74275 (from Delano and Lindsley 1982).

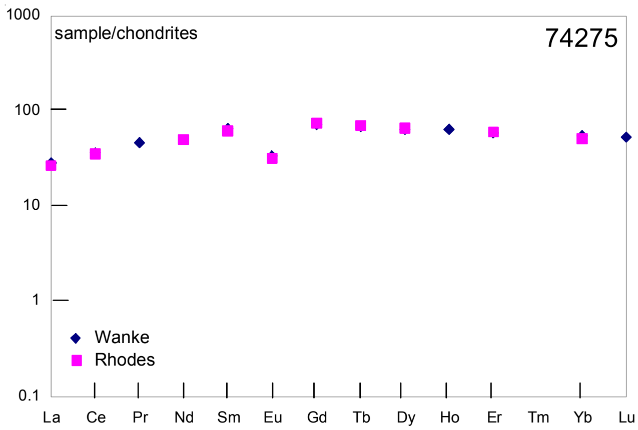

Figure 7: Normalized rare-earth-element diagram for 74275 (data from Wanke et al. 1974, Rhodes et al. 1976).

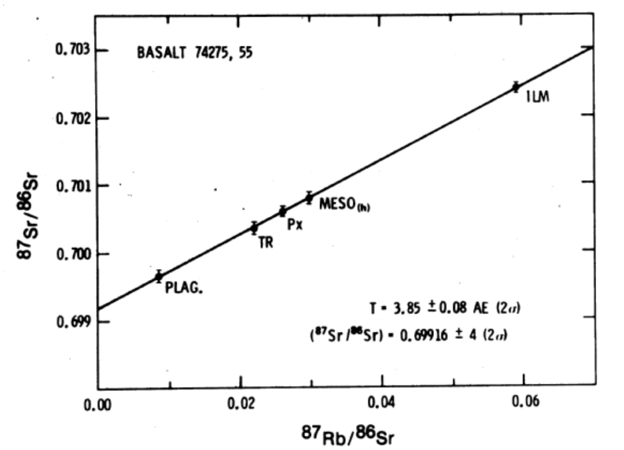

Figure 8: Rb-Sr isochron for 74275 (from Murthy and Coscio 1977).

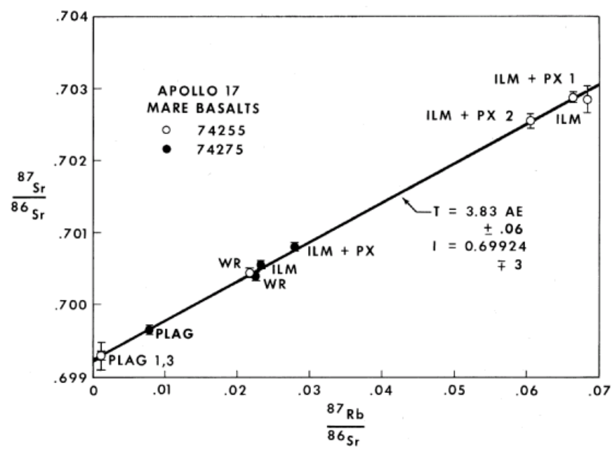

Figure 9: Rb-Sr isochron for 74255 with added data from 74275 (from Nyquist et al. 1976). The isochron fit for 74275 is 3.81 +/- 0.32 b.y.).

Unusual olivine with an "hourglass" structure has been reported by Hodges and Kushiro (1974).

Opaques: Armalcolite is rimmed with ilmenite (Hodges and Kushiro 1974; El Goresy et al. 1974). Small euhedral chromite are found as inclusions in the olivine clusters (Neal and Taylor 1993).

Chemistry

The chemical composition of 74275 has been determined by Duncan et al. (1974), Wanke et al. (1974), Rose et al. (1975) and other (table 1). Trace elements have been determined by Rhodes et al. (1976), Wanke et al. (1974) and others (table 1, figure 7). Dickenson et al. (1989) determined Ge, Gibson (1987), Petrowski et al. (1974), Reese and Thode (1974) and Des Maris (1980) determined S, C, N and H, Garg and Ehman (1976) and Hughes and Schmitt (1985) determined Zr and Hf.

Radiogenic age dating

Murthy and Coscio (1977) dated 74275 at 3.85 ± 0.08 b.y. using Rb-Sr (figure 8). Nyquist et al. (1976) obtained an age of 3.81 ± 0.32 b.y. (figure 9). Nunes et al. (1974) and Paces et al. (1991) determined whole rock U-Th-Pb and Sm-Nd isotopics, respectively.

Cosmogenic isotopes and exposure ages

Goswami and Lal (1974) determined a SUNTAN exposure age of 2.8 m.y. from the density and gradient of nuclear tracks caused by very heavy cosmic ray bombardment and this was initally thought to be the age of Shorty crater. Eugster et al. (1977) measured the isotopic ratio of all the rare gases and determined an "exposure age" of 32.2 ± 1.4 m.y. by the ^{81}Kr-Kr method for 74275. However, the age of Shorty crater (~19 m.y.) was determined from the samples of a nearby boulder, thus sample 74275 is thought to have had a complicated exposure history.

Fruchter et al. (1982), Klein et al. (1990) and Fink et al. (1998) have reported precise depth profiles of the cosmogenic radionuclides ^{10}Be, ^{22}Na, ^{26}Al and ^{41}Ca (figures 10-13) and modeled the flux and energy of cosmic rays. The ^{22}Na activity is residual from the 1972 solar flare event (Sisterson and Reedy 1997). Schnabel et al. (2000) used accelerator mass spectroscopy to determine a depth profile for ^{59}Ni , produced by SCR alpha particles in the very surface layer (figure 14). However, the erosion rate due to micrometeorite bombardment remains unknown for this sample.

Table 1. Chemical composition of 74275.

reference	Duncan 74		Rose 75		Rhodes 76		Wanke 74		Murthy 77		Miller 74			Hodges 74		Green 75	
weight											recalculated						
SiO2 %	38.43	(a)	38.44	(a)	- - - -		38.73				38.3	39.58	(c)	38.4	(d)	37.9	(d)
TiO2	12.66	(a)	12.75	(a)			11.71				11.88	8.75		14.1	(d)	12.6	(d)
Al2O3	8.51	(a)	8.93	(a)			8.4				8.51	9.07		8.5	(d)	8.3	(d)
FeO	18.25	(a)	18.03	(a)			18.29				18.31	18.18		17.4	(d)	19.1	(d)
MnO	0.247	(a)	0.27	(a)			0.241				0.25	0.25		0.35	(d)	0.2	(d)
MgO	10.26	(a)	10.46	(a)			10.16				10.47	10.14		8.6	(d)	10.4	(d)
CaO	10.38	(a)	10.26	(a)			10.08				10.36	10.08		10.7	(d)	10.2	(d)
Na2O	0.37	(a)	0.33	(a)			0.37				0.38	0.39		0.22	(d)	0.4	(d)
K2O	0.075	(a)	0.09	(a)			0.08		0.043	(b)				0.07	(d)	0.1	(d)
P2O5	0.074	(a)	0.06	(a)	Gibson		0.063										
S %	0.141	(a)			0.14												
sum																	
Sc ppm			78	(a)			74	(c)									
V	79	(a)	62	(a)													
Cr	4372	(a)	4447	(a)			3688	(c)									
Co	24	(a)	31	(a)			22.5	(c)									
Ni	<3	(a)	16	(a)			-										
Cu			40	(a)			3.5	(c)									
Zn			5.8	(a)			1.7	(c)									
Ga			6.2	(a)			3.4	(c)			Dickinson 89						
Ge ppb											6.8						
As ppb							4	(c)									
Se											Nyquist 76	Paces 91					
Rb	1.9	(a)			1.2	(b)	1.22	(c)	1.03	(b)	1.2	0.864					
Sr	158	(a)	152	(a)	153	(b)	195	(c)	134.9	(b)	153	116					
Y	81.5	(a)	116	(a)			79	(c)			Hughes 85						
Zr	248	(a)	290	(a)			246	(c)			261						
Nb	22.1	(a)					19	(c)									
Mo																	
Ru																	
Rh																	
Pd ppb																	
Ag ppb																	
Cd ppb																	
In ppb																	
Sn ppb																	
Sb ppb																	
Te ppb																	
Cs ppm							53	(c)									
Ba	89	(a)			67.3	(b)	83	(c)	73.83	(b)							
La					6.33	(b)	6.7	(c)									
Ce					21.4	(b)	22.1	(c)									
Pr							4.2	(c)				Paces 91					
Nd					22.8	(b)						22.5					
Sm					9.19	(b)	9.76	(c)				9.24					
Eu					1.8	(b)	1.91	(c)									
Gd					14.8	(b)	14.2	(c)									
Tb							2.5	(c)									
Dy					16.3	(b)	15.8	(c)									
Ho							3.6	(c)									
Er					9.66	(b)	9.4	(c)									
Tm																	
Yb			11		8.47	(b)	9.02	(c)									
Lu							1.3	(c)			Hughes 85						
Hf							8.33	(c)			8.4						
Ta							1.5	(c)									
W ppb							0.06	(c)									
Re ppb							<0.5	(c)									
Os ppb																	
Ir ppb																	
Pt ppb																	
Au ppb							0.19	(c)			Nunes 74						
Th ppm											0.4654	(b)					
U ppm							0.16	(c)			0.136	(b)					

technique (a) XRF, (b) IDMS, (c) INAA, (d) fused bead, elc. Probe

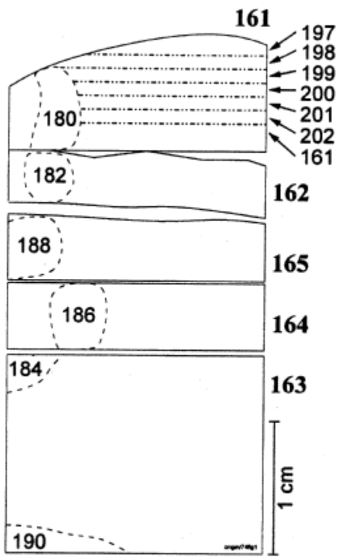

Figure 10: Schematic drawing of column cut from 74275 for study of cosmogenic radionuclide production from energetic solar cosmic ray (from Fink et al. 1998).

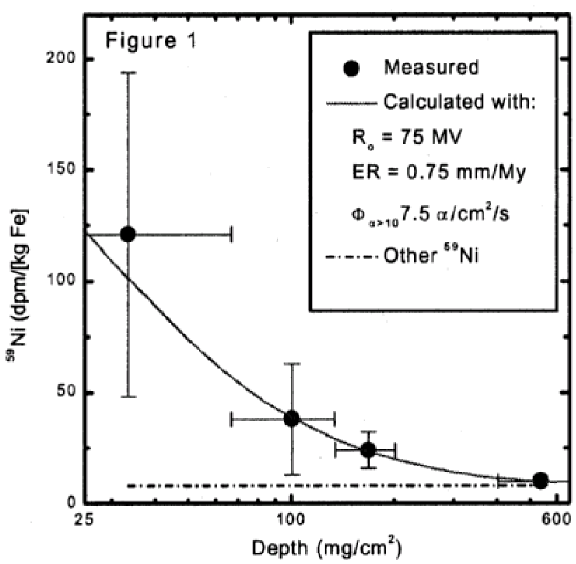

Figure 14: Ni 59 depth profile of very surface of 74275 (from Schnabel et al. 2000) due to irradiation by solar alpha particles.

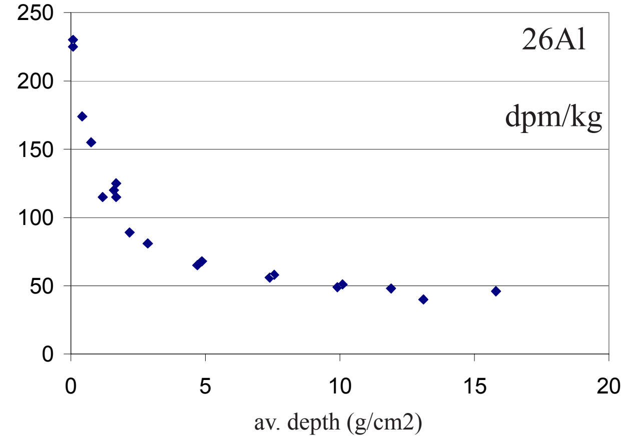

Figure 11: Al 26 depth profile for 74275 (from data by Fruchter et al. (1982); Klein et al (1988); Fink et al. (1998).

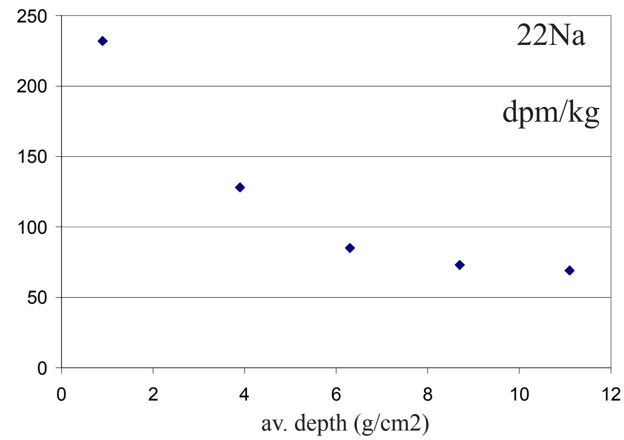

Figure 12: Na 22 depth profile for 74275 (from data by Fruchter et al. (1982) due to irradiation by 1972 solar flare (Sisterson and Reedy 1997).

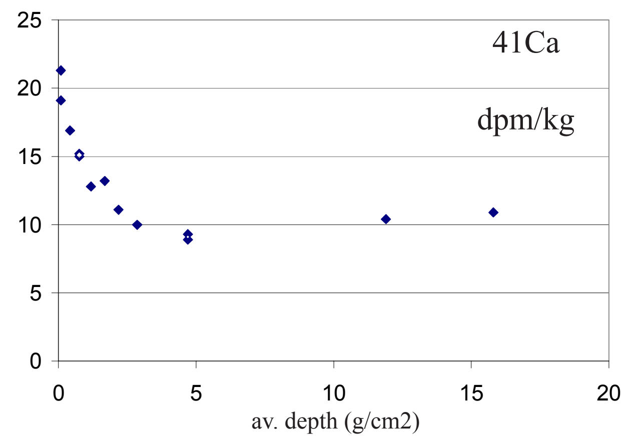

Figure 13: Ca 41 depth profile for 74275 (from data by Fink et al. 1998).

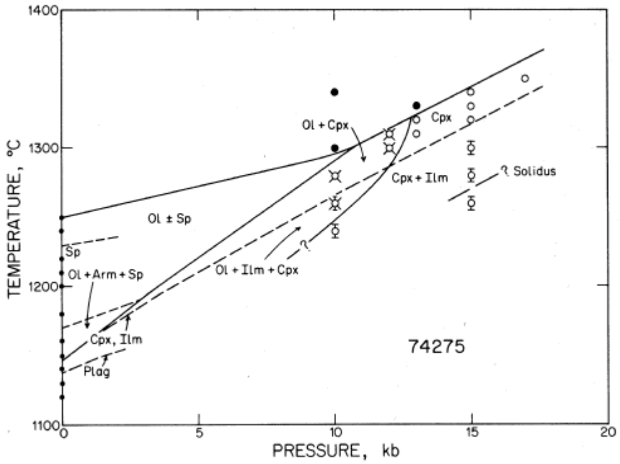

Figure 15: Experimentally determined phase relations as function of pressure for 74275 (from Green et al. 1975).

Other Studies

74275 is one of the most Mg rich of the high-Ti Apollo samples, and for this reason the composition of 74275 became the starting point for high-pressure phase-relation experiments (figure 15) aimed at determining the depth of origin of high-Ti mare basalt (Green et al. 1974, 1975; Walker et al. 1976; Delano and Lindsey 1982). However, 74275 contains olivine inclusions that are too mg* to have crystallized from the melt they are in, and the bulk composition of 74275 may not represent the composition of a true melt.

Additional experiments on 74275 include element partioning between phases (Irving et al. 1978), cooling rate and nucleation (Usselman and Lofgren 1976) and the effects of oxygen fugacity and stability of armalcolite (O'hara and Humphries 1975; Satan and Taylor 1979).

The magnetic properties of 74275 have been studied by Brecher et al. (1974); Pearce et al. (1974); and Nagata et al. (1975).

Mizutani and Osako (1974) determined the compressional and shear wave velocity as a function of pressure using a sample of 74275.

Processing

Two partial slabs and two columns (4 cm deep) were cut from this sample. The first partial slab (,13 to ,34) was cut in 1973 (figure 16). A second slab (,166 and ,167) and a column (,161 top; to ,165 middle) was cut in 1981 (figure 17). A second column was cut from ,166 in 1998. Apparently the big piece ,2 broke in storage. A documented surface piece ,159 can be identified in the center of the top surface.

There are 17 thin sections.

List of Photos #
S73-16018 to 16024 Color PET
S73-19156 to 19171 B&W PET
S81-34492 to 34494
S98-02167 to 02174

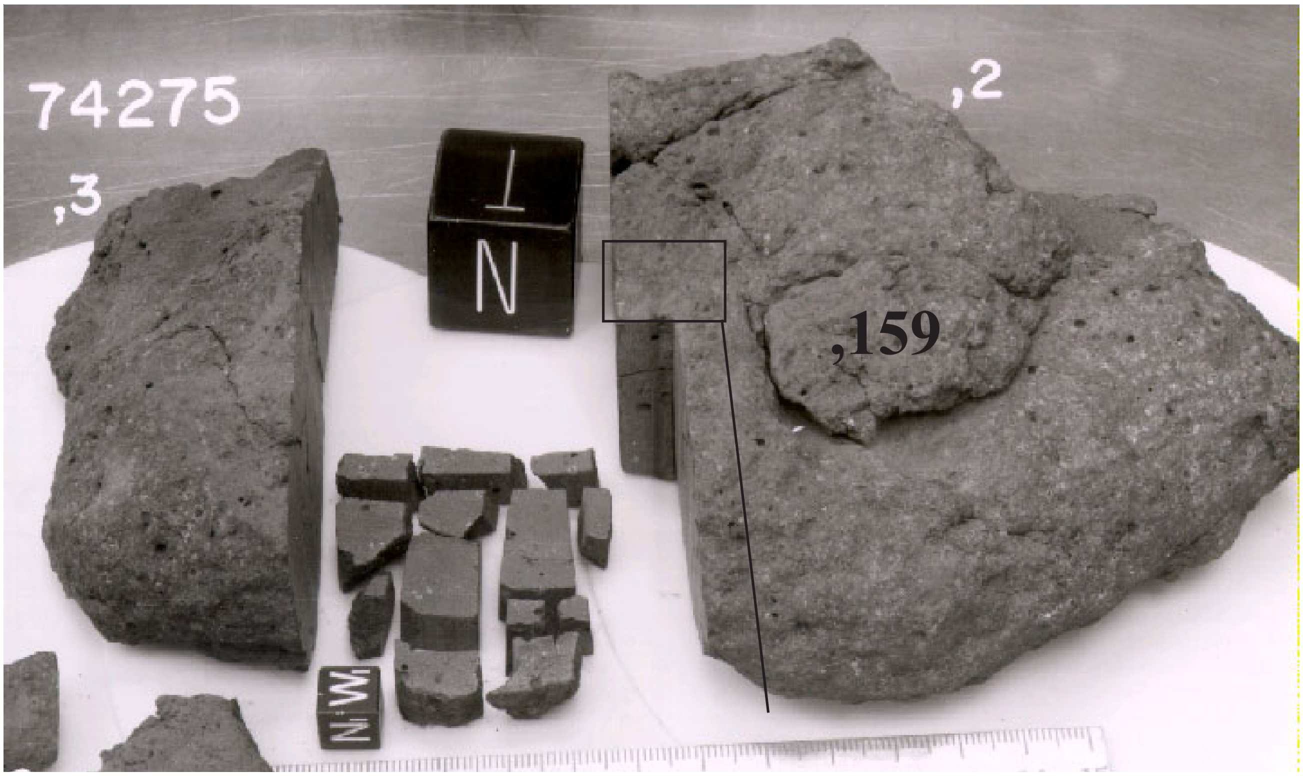

Figure 16: First partial slab cut from 74275. Positon of first column and second slab indicted. NASA# 73-28789. Nice illustration of our 1 cm cube as well as our 1 inch cube!

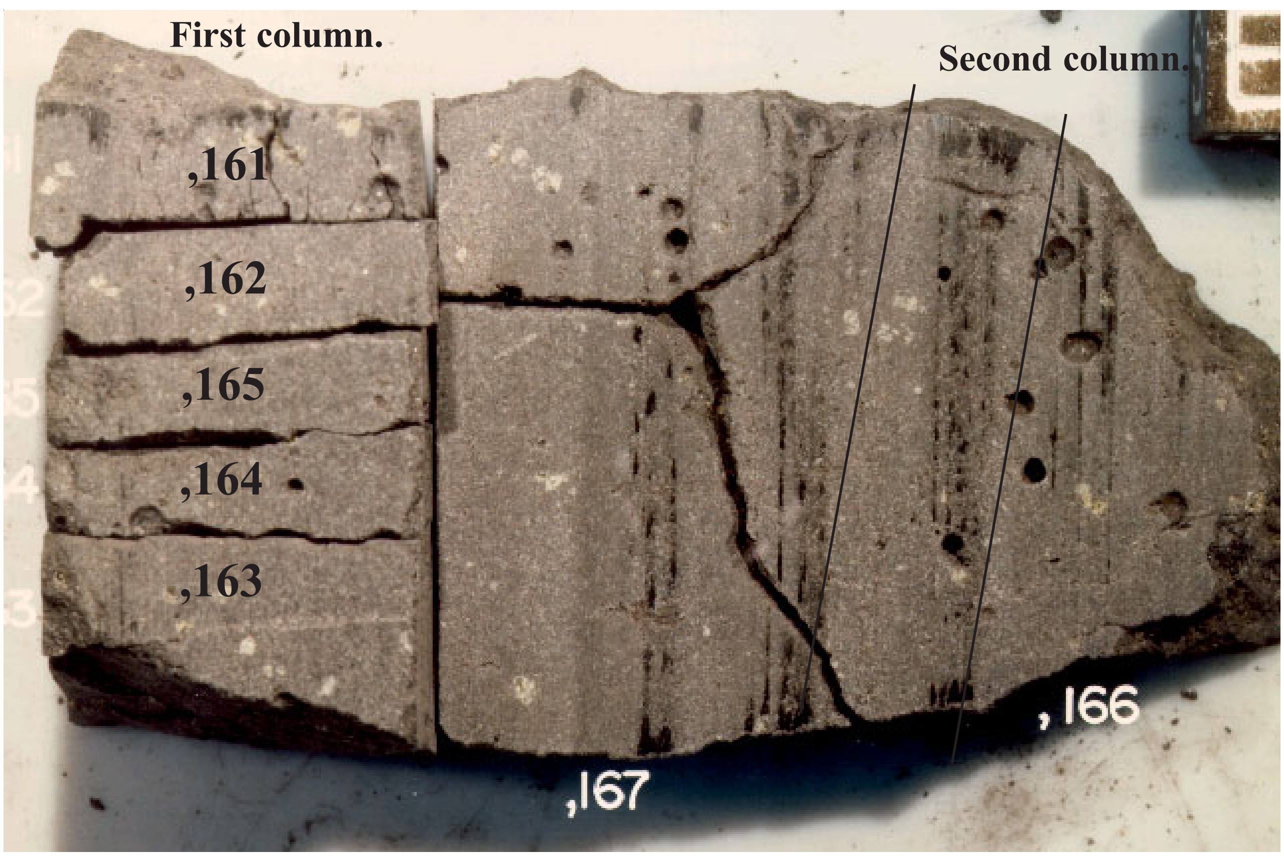

Figure 17: Second slab and first column cut from 74275. Approximate positon of second column shown. NASA# S81-34494.